Inorg. Chem. **2007**, *46*, 6483–6494

Platinum Acetylide Two-Photon Chromophores

Joy E. Rogers,[†,‡] Jonathan E. Slagle,[†,§] Douglas M. Krein,[†,||] Aaron R. Burke,[†,||] Benjamin C. Hall,[†,⊥] Albert Fratini,[†,#] Daniel G. McLean,[†,+] Paul A. Fleitz,[†] Thomas M. Cooper,*[,†] Mikhail Drobizhev,[£] Nikolay S. Makarov,[£] Aleksander Rebane,*[,£] Kye-Young Kim,[▽] Richard Farley,[▽] and Kirk S. Schanze*[,▽]

Materials and Manufacturing Directorate, Air Force Research Laboratory, Wright-Patterson Air Force Base, Ohio 45433, UES, Inc., Dayton, Ohio 45432, AT&T Government Solutions, Dayton, Ohio 45324, General Dynamics Information Technology, Dayton, Ohio 45431, Universal Technology Corporation, Dayton, Ohio 45432, Department of Chemistry, University of Dayton, Dayton, Ohio 45469, Science Applications International Corporation, Dayton, Ohio 45431, Physics Department, Montana State University, Bozeman, Montana 59717, and Department of Chemistry, University of Florida, Gainesville, Florida 32611

Received March 22, 2007

To explore the photophysics of platinum acetylide chromophores with strong two-photon absorption cross-sections, we have investigated the synthesis and spectroscopic characterization of a series of platinum acetylide complexes that feature highly π-conjugated ligands substituted with π-donor or -acceptor moieties. The molecules (numbered **1**–**4**) considered in the present work are analogs of bis(phenylethynyl)bis(tributylphosphine)platinum(II) complexes. Molecule **1** carries two alkynyl-benzothiazolylfluorene ligands, and molecule **2** has two alkynyl-diphenylaminofluorene ligands bound to the central platinum atom. Compounds **3** and **4** possess two dihexylaminophenyl substituents at their ends and differ by the number of platinum atoms in the oligomer "core" (one vs two in **3** and **4**, respectively). The ligands have strong effective two-photon absorption cross-sections, while the heavy metal platinum centers give rise to efficient intersystem crossing to long-lived triplet states. Ultrafast transient absorption and emission spectra demonstrate that one-photon excitation of the chromophores produces an S_1 state delocalized across the two conjugated ligands, with weak (excitonic) coupling through the platinum centers. Intersystem crossing occurs rapidly ($k_{isc} \approx 10^{11}$ s^{-1}) to produce the T_1 state, which is possibly localized on a single conjugated fluorenyl ligand. The triplet state is strongly absorbing ($\epsilon_{TT} > 5 \times 10^4$ M^{-1} cm^{-1}), and it is very long-lived ($\tau > 100$ μs). Femtosecond pulses were used to characterize the two-photon absorption properties of the complexes, and all of the chromophores are relatively efficient two-photon absorbers in the visible and near-infrared region of the spectrum (600–800 nm). The complexes exhibit maximum two-photon absorption at a shorter wavelength than 2λ for the one-photon band, consistent with the dominant two-photon transition arising from a two-photon-allowed gerade–gerade transition. Nanosecond transient absorption experiments carried out on several of the complexes with excitation at 803 nm confirm that the long-lived triplet state can be produced efficiently via a sequence involving two-photon excitation to produce S_1, followed by intersystem crossing to produce T_1.

Introduction

Interest in two-photon absorbing materials has increased within the past decade because of their usefulness in various applications. They are being developed for use in optical data storage,[1,2] frequency upconverted lasing,[3−5] nonlinear photonics,[6−8] microfabrication,[9,10] fluorescence imaging,[11]

* To whom correspondence should be addressed. E-mail: Thomas.Cooper@wpafb.af.mil (T.M.C.); rebane@physics.montana.edu (A.R.); kschanze@chem.ufl.edu (K.R.S.).
† Wright-Patterson Air Force Base.
‡ UES, Inc..
§ AT&T Government Solutions.
|| General Dynamics Information Technology.
⊥ Universal Technology Corporation.
University of Dayton.
+ Science Applications International Corporation.
£ Montana State University.
▽ University of Florida.

(1) Parthenopoulos, D. A.; Rentzepis, P. M. *Science* **1989**, *249*, 843.
(2) Dvornikov, A. S.; Rentzepis, P. M. *Opt. Commun.* **1995**, *119*, 341.
(3) Bhawalkar, J. D.; He, G. S.; Prasad, P. N. *Rep. Prog. Phys.* **1996**, *59*, 1041.
(4) He, G. S.; Zhao, C. F.; Bhawalkar, J. D.; Prasad, P. N. *Appl. Phys. Lett.* **1995**, *78*, 3703.
(5) Zhao, C. F.; He, G. S.; Bhawalkar, J. D.; Park, C. K.; Prasad, P. N. *Chem. Mater.* **1995**, 7, 1979.
(6) Fleitz, P. A.; Sutherland, R. A.; Strogkendl, F. P.; Larson, F. P.; Dalton, L. R. *SPIE Proc.* **1998**, *3472*, 91.
(7) He, G. S.; Bhawalkar, J. D.; Zhao, C. F.; Prasad, P. N. *Appl. Phys. Lett.* **1995**, *67*, 2433.

10.1021/ic700549n CCC: $37.00
Published on Web 07/10/2007

and photodynamic therapy.[12] Two-photon absorption (2PA) of two lower-energy photons results in initiation of the same photophysical processes as one-photon absorption (1PA) of one high-energy photon. This is advantageous for two reasons. First, by using lower-energy photons, a material will be protected from photodegradation effects. Second, the quadratic dependence of 2PA on intensity causes photochemistry to take place in a small focal region, allowing for more control in microfabrication and imaging applications.

A generally accepted 2PA material design strategy is to develop chromophores with large changes in polarization upon excitation.[13] This is achieved through either D−π−A (donor group−π-conjugated group−acceptor group), D−π−D, or A−π−A structural motifs, and many such materials have been designed, showing remarkable increases in 2PA cross-sections.[14−23] For many of these chromophores, there is a large variation in the "effective" 2PA cross-section obtained by using differing pulse widths. A dramatic enhancement of this value in the nanosecond, compared to that in the femtosecond, regime has been repeatedly observed.[24] This enhanced loss in nonlinear transmission when using nanosecond pulses is attributed to contributions from the excited-state absorption.[8,25] Recently, we confirmed that this effect in AFx chromophores is indeed caused by absorption from both the singlet and triplet excited states.[26,27]

In the literature, there are several examples of Pt acetylides that exhibit 2PA in the visible or near-IR regions. In particular, bis((4-phenylethynyl)phenyl)ethynyl)bis-(tributylphosphine)platinum(II) (**PE2)** has a measurable intrinsic (femtosecond) 2PA cross-section (σ_2) of 7 GM at 720 nm.[32,40,41] The 2PA coefficient (β) of this molecule was first reported at 595 nm to be 0.34 cm/GW, which corresponds to 235 GM for σ_2.[28,42] The latter measurement was made using picosecond pulses, which allows for considerable excited-state absorption from both the S_1 and the T_1 excited states. This would correctly be termed an effective 2PA cross-section. More recently, a dendron-decorated **PE2** series has been studied and shown to have similar intrinsic σ_2 values at 720 nm.[43] Platinum acetylides substituted with thiophene groups in place of phenyl groups have also shown a doubling of the intrinsic σ_2 value at 740 nm.[40,41]

In the present investigation, we describe chromophores (**1**−**4**) that have strong 2PA and undergo rapid singlet → triplet intersystem crossing to afford a large triplet excited-state population. Because the triplet-state lifetime is long relative to a nanosecond laser pulse, these materials exhibit enhanced nonlinear absorption resulting from the triplet−triplet absorption. The systems which are the focus of this investigation incorporate one or more platinum(II) centers. Platinum is used because of its large spin−orbit coupling which gives rise to rapid intersystem crossing and high effective triplet yields. Shown in Figure 1 are the structures of the Pt complexes **1**−**4**, **PE2**, and the ligands. Molecule **1** carries two benzothiazolylfluorene units, and molecule **2** carries two diphenylaminofluorene substituents. The design is based on the well-known D−π−D or A−π−A motifs, yielding materials that have significant near-IR 2PA strength. Chromophores **3** and **4** are based on the same D−π−D concept but include an additional phenyl acetylene group.

(8) Ehrlich, J. E.; Wu, X. L.; Lee, L. Y.; Hu, Z. Y.; Roeckel, H.; Marder, S. R.; Perry, J. *Opt. Lett.* **1997**, *22*, 1843.
(9) Kawata, S.; Sun, H. B.; Tanaka, T.; Takada, K. *Nature* **2001**, *412*, 697.
(10) Cumpston, B. H.; Ananthavel, S. P.; Barlow, S.; Dyer, D. L.; Ehrlich, J. E.; Erskine, L. L.; Heikal, A. A.; Kuebler, S. M.; Le, I. Y. S.; McCord-Maughon, D.; Qin, J.; Rockel, H.; Rumi, M.; Wu, X. L.; Marder, S. R.; Perry, J. *Nature* **1999**, *398*, 51.
(11) Denk, W.; Strickler, J. J.; Webb, W. W. *Science* **1990**, *248*, 73.
(12) Bhawalkar, J. D.; Kumar, N. D.; Zhao, C. F.; Prasad, P. N. *J. Clin. Laser Med. Surg.* **1997**, *15*, 201.
(13) Marder, S. R.; Gorman, C. B.; Meyers, F.; Perry, J.; Bourhill, G.; Bredas, J.-L.; Pierce, B. M. *Science* **1994**, *265*, 632.
(14) Prasad, P. N.; Reinhardt, B. A. *Chem. Mater.* **1990**, *2*, 660.
(15) Larson, E. J.; Friesen, L. A.; Johnson, C. K. *Chem. Phys. Lett.* **1997**, *265*, 161.
(16) Albota, M.; Beljonee, D.; Bredas, J.-L.; Ehrlich, J. E.; Fu, J.-Y.; Heikal, A. A.; Hess, S. E.; Kogej, T.; Levin, M. D.; Marder, S. R.; McCord-Maughon, D.; Perry, J.; Rockel, H.; Rumi, M.; Subramanian, G.; Webb, W. W.; Wu, X. L.; Xu, C. *Science* **1998**, *281*, 1653.
(17) Chung, S. J.; Kim, K. S.; Lin, T. C.; He, G. s.; Swiatkiewicz, J.; Prasad, P. N. *J. Phys. Chem. B* **1999**, *103*, 10741.
(18) Oberle, J.; Bramerie, L.; Jonusauskas, G.; Rullier, C. *Opt. Commun.* **1999**, *169*, 325.
(19) Belfield, K. D.; Hagan, D. J.; Van Stryland, E. W.; Schafer, K. J.; Negres, R. A. *Org. Lett.* **1999**, *1*, 1575.
(20) Kannan, R.; He, G. S.; Yuan, L.; Xu, F.; Prasad, P. N.; Dombroskie, A. G.; Reinhardt, B. A.; Baur, J. W.; Vaia, R. A.; Tan, L. S. *Chem. Mater.* **2001**, *13*, 1896.
(21) Mongrin, O.; Porres, L.; Katan, C.; Pons, T.; Mertz, J.; Blanchard-Desce, M. *Tetrahedron Lett.* **2003**, *44*, 8121.
(22) Brousmiche, D. W.; Serin, J. M.; Frechet, J. M. J.; He, G. S.; Lin, T. C.; Chung, S. J.; Prasad, P. N. *J. Am. Chem. Soc.* **2003**, *125*, 1448.
(23) Marder, S. R. *Chem. Commun.* **2006**, *131*.
(24) Rumi, M.; Ehrlich, J. E.; Heikal, A. A.; Perry, J. W.; Barlow, S.; Hu, Z. Y.; McCord-Maughon, D.; Parker, T. C.; Rockel, H.; Thayumanavan, S.; Marder, S. R.; Beljonne, D.; Bredas, J.-L. *J. Am. Chem. Soc.* **2000**, *122*, 9500.
(25) Kleinschmidt, J.; Rentsh, S.; Tottleben, W.; Wilhelmi, B. *Chem. Phys. Lett.* **1974**, *24*, 133.
(26) Sutherland, R. L.; Brant, M. C.; Heinrichs, J.; Rogers, J. E.; Slagle, J. E.; McLean, D. G.; Fleitz, P. A. *J. Opt. Soc. Am. B* **2005**, *22*, 1939.
(27) Sutherland, R. L.; McLean, D. G.; Brant, M. C.; Rogers, J. E.; Fleitz, P. A.; Urbas, A. M. *SPIE Proc.* **2006**, *6330*, 633006.
(28) Staromlynska, J.; McKay, T. J.; Bolger, J. A.; Davy, J. R. *J. Opt. Soc. Am. B* **1998**, *15*, 1731.
(29) Rogers, J. E.; Cooper, T. M.; Fleitz, P. A.; Glass, D. J.; McLean, D. G. *J. Phys. Chem. A* **2002**, *106*, 10108.
(30) Liu, Y.; Jiang, S.; Glusac, K.; Powell, D. H.; Anderson, D. F.; Schanze, K. S. *J. Am. Chem. Soc.* **2002**, *124*, 12412.
(31) Haskins-Glusac, K.; Ghiviriga, I.; Abboud, K. A.; Schanze, K. S. *J. Phys. Chem. B* **2004**, *108*, 4969.
(32) Glimsdal, E.; Eriksson, A.; Vestberg, R.; Malmstrom, E.; Lindgren, M. *SPIE Proc.* **2005**, *5934*, 1.
(33) Reinhardt, B. A.; Brott, L. L.; Clarson, S. J.; Dillard, A. G.; Bhatt, J. C.; Kannan, R.; Yuan, L.; He, G. S.; Prasad, P. N. *Chem. Mater.* **1998**, *10*, 1863.
(34) Anemian, R.; andraud, C.; Nunzi, J.-M.; Morel, Y.; Baldeck, P. L. *SPIE Proc.* **2000**, *4106*, 329.
(35) Schroeder, R.; Ullrich, B. *Opt. Lett.* **2002**, *27*, 1285.
(36) Lee, K. S.; Yang, H.-K.; Lee, J.-H.; Kim, O.-K.; Woo, H. Y.; Choi, H.; Cha, M.; Blanchard-Desce, M. *SPIE Proc.* **2003**, *4991*, 175.
(37) Kannan, R.; He, G. S.; Lin, T. C.; Prasad, P. N.; Vaia, R. A.; Tan, L. S. *Chem. Mater.* **2004**, *16*, 185.
(38) Ma, W.; Wu, Y.; Han, J.; Gu, D.; Gan, F. *Chem. Phys. Lett.* **2005**, *403*, 405.
(39) Lin, T. C.; He, G. S.; Zheng, Q.; Prasad, P. N. *J. Mat. Chem.* **2006**, *16*, 2490.
(40) Glimsdal, E.; Carlsson, M.; Eliasson, B.; Lindgren, M. *SPIE Proc.* **2006**, 6401.
(41) Glimsdal, E.; Carlsson, M.; Eliasson, B.; Minaev, B.; Lindgren, M. *J. Phys. Chem. A* **2007**, *111*, 244.
(42) McKay, T. J.; Staromlynska, J.; Wilson, P.; Davy, J. R. *J. Appl. Phys.* **1999**, *85*, 1337.
(43) Vestberg, R.; Westlund, R.; Ericksson, A.; Lopes, C.; Carlsson, M.; Eliasson, B.; Glimsdal, E.; Lindgren, M.; Malmstrom, E. *Macromolecules* **2006**, *39*, 2238.

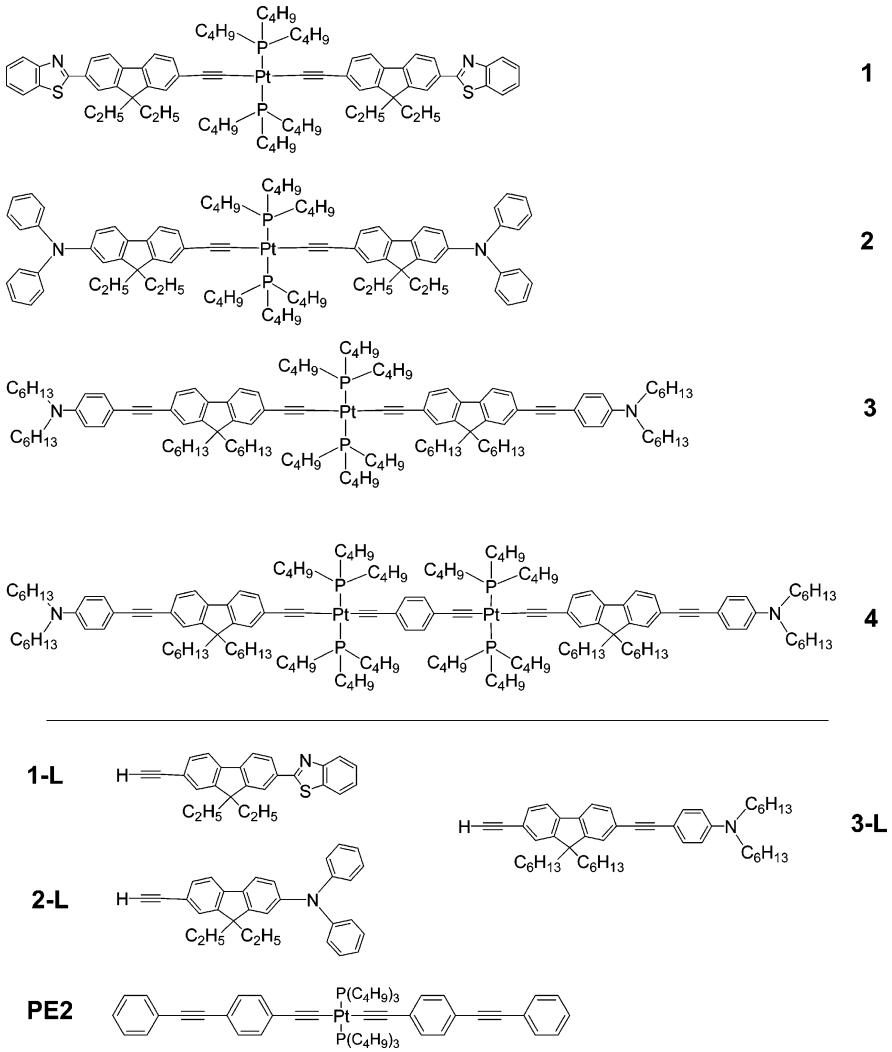

Figure 1. Chemical structures of platinum containing two-photon absorbing complexes **1**, **2**, **3**, and **4**, corresponding ligands **1-L**, **2-L**, and **3-L**, and **PE2**.

Complex **4** contains a Pt−C≡C−phenyl−C≡C−Pt unit in the "core" of the oligomer. This material was prepared to explore whether the triplet state properties would be influenced by the presence of a central ligand. Each of these structures is based on a series of oligomeric and polymeric platinum acetylides that we and others have previously studied but they contain ligands that are designed specifically to feature large 2PA cross-sections.[28−32] The ligand structures were developed on the basis of previous work which shows that very similar chromophores are effective two-photon-absorbing dyes.[19,20,33−39]

We show the chromophores depicted in Figure 1 exhibit a remarkable increase in the 2PA cross-section (σ_2) over **PE2** mentioned above. We present the photophysical properties of these materials as shown in the Jablonski diagram in Scheme 1 and discuss their structure−property relationships in terms of both 1PA and 2PA properties. The chromophores undergo efficient two-photon excitation to the S_1 (or higher) state with red or near-IR photons and then undergo intersystem crossing with near unit quantum yield to the triplet excited state. We show that, for these materials, the photophysical processes are the same for either one- or two-photon excitation.

Experimental Section

Synthesis. Chromophores **1** and **2** were synthesized at Air Force Research Laboratory (AFRL), and chromophores **3** and **4** were synthesized at University of Florida (UF). Details on the synthesis of these materials are given in the Supporting Information.

General Techniques. Ground state UV−vis absorption spectra were measured in 1 cm quartz cuvettes on either a Cary 100 (UF) or a Cary 500 (AFRL) spectrophotometer. Corrected steady-state emission spectra were measured using either a Perkin-Elmer model LS 50B fluorometer (AFRL) or a SPEX F-112 fluorometer (UF). Samples were placed in 1 cm quartz cuvettes, and the optical density was adjusted to approximately 0.1 at the excitation wavelength. Time-correlated single-photon counting (Edinburgh Instruments OB 920 Spectrometer) was used to determine fluorescence lifetimes (AFRL). The samples were pumped using a 70 ps laser diode either at 401 nm or at 375 nm. Emission was detected on a cooled microchannel plate PMT. Data was analyzed using a reconvolution software package provided by Edinburgh Instruments. Nanosecond time-resolved absorption spectra at UF were obtained on an instrument that has been previously described that uses the third harmonic of a Nd:YAG laser (Spectra Physics GCR-14, 355 nm, 10 ns fwhm, 10 mJ pulse^{-1}, 20 mJ cm^{-2} irradiation) as excitation source.[44] Samples were deoxygenated by bubbling with nitrogen.

(44) Wang, Y. S.; Schanze, K. S. *Chem. Phys.* **1993**, *176*, 305.

Scheme 1. Energy Level Diagram and Summary of Spectroscopic Measurements[a]

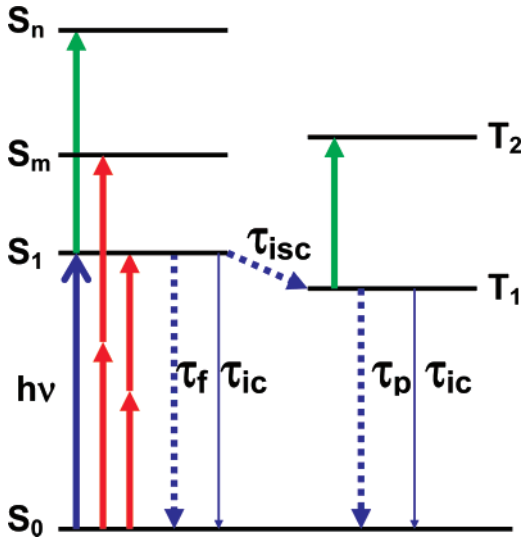

[a] The chromophore undergoes one-photon excitation from the ground state (S_0) to the S_1 state (blue arrow). The excitation can occur by linear, femtosecond, or nanosecond excitation. The S_1 state undergoes emissive decay to the ground state by fluorescence (τ_f, dotted blue arrow) or internal conversion (τ_{ic}, solid blue arrow) or undergoes intersystem crossing to the T_1 state (τ_{isc}, dotted blue arrow). When a femtosecond pump−probe experiment is being performed, the probe beam causes the S_1 state to undergo a second one-photon excitation to the S_n state, along with observation of intersystem crossing. Two-photon excitation from S_0 can go to either the S_1 state or the S_m state (red arrow). When a nanosecond pump−probe experiment is being performed, the intersystem crossing process occurs within the laser pulse time. The T_1 state undergoes one-photon excitation to the T_n state (green arrow) or decays to the ground state by phosphorescence (τ_p, dotted blue line) or internal conversion (τ_{ic}, solid blue line).

Nanosecond transient absorption measurements (AFRL) were carried out using the third harmonic (355 nm) of a Q-switched Nd:YAG laser (Quantel Brilliant, pulse width ~5 ns). Pulse fluences of up to 4 mJ cm^{-2} at the excitation wavelength were typically used. A detailed description of the laser flash photolysis apparatus was published earlier.[29] All samples were deoxygenated by three successive freeze−pump−thaw cycles. Two-photon pumped transient absorption (AFRL) used the same laser flash photolysis apparatus, but the samples were pumped with the idler beam (803 nm) of a 355 nm optical parametric oscillator (OPO). Color filters removed the signal beam and residual 355 nm radiation and were verified. The idler beam was focused into the sample transverse to the white light probe with an energy of 4 mJ at 803 nm. Samples were made at concentrations of 0.02 M and degassed by three cycles of freeze−pump−thaw. The probe was masked at 1 mm by 1 cm at the front and rear face of the cuvette and imaged onto a 625 μm slit of a monochromator. The probe image could then be translated across the slit to a point just off the focus of the laser, producing a transient spectrum.

Ultrafast transient absorption measurements were performed using a modified version of the femtosecond pump−probe UV−vis spectrometer described elsewhere.[45] Briefly, 1 mJ, 100 fs pulses at 800 nm at 1 kHz repetition rate were obtained from a diode-pumped Ti:Sapphire regenerative amplifier (Spectra Physics Hurricane). The output laser beam was split into pump and probe (85 and 15%) by a beam splitter. The pump beam was directed into a frequency doubler (400 nm) (CSK Super Tripler) and then was focused into the sample. The probe beam was delayed in a computer-controlled optical delay (Newport MM4000 250 mm linear positioning stage) and then focused into a sapphire plate to generate white light continuum. The white light was then overlapped with the pump beam in a 2 mm quartz cuvette and coupled into a CCD detector (Ocean Optics S2000 UV−vis). Data acquisition was controlled by software developed by Ultrafast Systems LLC. The chirp effect on the spectra were within experimental error, so no chirp corrections were made.

Fluorescence quantum yields were determined using the actinometry method previously described.[29] For **1**, **2**, **1-L**, and **2-L,** quinine sulfate was used as an actinometer with a known fluorescence quantum yield of 0.55 in 1.0 N H_2SO_4.[46] These samples were excited at 330 (**1-L** and **2-L**) or 370 nm (**1** and **2**) with a matched optical density of 0.1. The fluorescence quantum yield for **3-L** was measured relative to Coumarin 30 in CH_3CN where $\phi = 0.67$.[47] Emission quantum yields for **3** and **4** are reported relative to Ru(bpy)$_3$ in air-saturated water for which $\phi = 0.0379$, and an appropriate correction was applied for the difference in refractive indices of actinometer and sample solvent.[48] The triplet molar absorption coefficients of the four Pt compounds were determined using relative actinometry. Benzophenone was used as the actinometer with a known molar absorption coefficient of $\Delta\epsilon_{525nm} = 7870 \pm 1200$ M^{-1} cm^{-1} and a triplet quantum yield of $\Phi_T = 1.0$.[49,50] Matched optical densities of 0.8 of **1**, **2**, **3**, **4**, and benzophenone at 355 nm were used in each determination. While the o.d. is higher than normally used with a right-angle geometry, inner filter effects were avoided by the geometry for the collection of the probe beam light. Data were obtained at various laser fluence ranges to pinpoint useful ranges in the data where nonlinear effects were not occurring. The linear working range was usually 0−500 μJ cm^{-2} for Pt complexes and up to ~4 mJ cm^{-2} for benzophenone. ΔA at each energy was determined and then plotted as a function of laser fluence for both the unknown samples and the benzophenone. The following expression (eq 1) was used to obtain $\Delta\epsilon_{sam}$ of the sample:

$$\Delta\epsilon_{sam} = \frac{\text{slope}_{sam}\Phi_{ISCref}\Delta\epsilon_{ref}}{\text{slope}_{ref}\Phi_{ISCsam}} \quad (1)$$

The quantities slope$_{sam}$ and slope$_{ref}$ are the respective slopes, Φ_{ISCref} and Φ_{ISCsam} are the known intersystem crossing quantum yields of both the reference and the sample, and $\Delta\epsilon_{ref}$ is the known molar absorption coefficient of the benzophenone.

Quantum yields for intersystem crossing were determined at UF using the method of photoacoustic calorimetry (PAC). Details on the PAC methods and instrumentns have been previously described.[51] Ferrocene was used as a calorimetric reference sample. Ferrocene releases heat with unit efficiency after excitation. All samples were degassed with nitrogen for 15 min, and the measurements were taken under a nitrogen atmosphere. The data were taken at various laser fluences to minimize the nonlinear absorption effects. The linear laser power range was 0−30 μJ/pulse, and the beam was focused through a 2.0 mm slit. The pressure wave produced after laser excitation was detected through a piezoelectric transducer with 1 MHz bandwidth. The amplitude of each wave is plotted versus laser energy. The ratio of the slopes represents ϕ_p.

(45) Nikolaitchik, A. V.; Korth, O.; Rodgers, M. A. J. *J. Phys. Chem. A* **1999**, *103*, 7587.
(46) Demas, J. N.; Crosby, G. A. *J. Phys. Chem.* **1971**, *75*, 991.
(47) Jones II, G.; Jackson, W. R.; Choi, C.; Bergmark, W. R. *J. Phys. Chem.* **1985**, *89*, 294.
(48) Thorn, N. B. *Chromophore Quencher-Based Luminescence Probes for DNA*; University of Florida: Gainesville, FL, 1995.
(49) Carmichael, I.; Helman, W. P.; Hug, G. L. *J. Phys. Chem. Ref. Data* **1987**, *16*, 239.
(50) Amand, B.; Bensasson, R. *Chem. Phys. Lett.* **1975**, *34*, 44.
(51) Walters, K. A.; Schanze, K. S. *Spectrum* **1998**, *11*, 1.

Intersystem crossing quantum yields (Φ_{ISC}) were obtained from eq 2.

$$(\phi_p)(E_{h\nu}) = (E_{h\nu} - E_S) + (1 - \Phi_{ISC} - \Phi_F)E_S + \Phi_{ISC}(E_S - E_T) \quad (2)$$

Where ϕ_p is the fraction of the heat produced by the sample relative to the heat evolved by the reference solution, $E_{h\nu}$ is the energy that corresponds to excitation wavelength (355 nm = 80.5 kcal), E_S is the energy of singlet excited-state of the sample, and E_T is the energy of triplet excited-state of the sample. Nonradiative decay of T_1 to S_0 is not considered in this calculation because PAC cannot measure heat release on longer time scales such as tens of microseconds (triplet state) because of the 1 MHz frequency bandwidth of the transducer. As a control experiment, Φ_{ISC} of benzophenone and anthracene were measured using ferrocene as an actinometer. The Φ_{ISC} of benzophenone and anthracene are 0.96 and 0.78, respectively. These numbers are within ±10% range compared to the previously reported value: $\Phi_{ISC} = 1$ for benzophenone[50,52] and $\Phi_{ISC} = 0.71$ for anthracene.[53]

The laser system for two-photon absorption measurements, performed at Montana State University, comprised a Ti:sapphire femtosecond oscillator (Coherent Mira 900) pumped by 5 W CW frequency-doubled Nd:YAG laser (Coherent Verdi) and a 1-kHz repetition rate Ti:sapphire femtosecond regenerative amplifier (Clark MXR CPA-1000). The pulses from the amplifier were down-converted with an optical parametric amplifier, OPA (Quantronix TOPAS), whose output can be continuously tuned from 1100 to 2200 nm. The second harmonic of signal and idler was used for two-photon excitation in $\lambda_{ex} = 550-800$ and 800−1100 nm regions, respectively. The OPA output signal pulse energy was 100−200 μJ (20−30 μJ after frequency doubling of signal and 5−10 μJ after frequency doubling of idler), and the pulse duration was 100 fs. The pulse energy and beam size at the sample were $E_{ex} = 5-20$ μJ and $d = 300-500$ μm, respectively.

The linearly polarized excitation laser beam was slightly focused with an $f = 25$ cm cylindrical lens onto the sample solution contained in a 1 cm spectroscopic cell and placed 15 cm behind the lens. A small fraction of the beam was split off by a thin glass plate placed just before the sample and directed to the reference detector (Molectron). The sample fluorescence was collected in frontal geometry with a spherical mirror ($f = 50$ cm, diameter $d =$ 10 cm) and focused with magnification ratio of ~1 on the entrance slit of an imaging grating spectrometer (Jobin Yvon Triax 550). The 2PA spectrum (in relative units) was obtained by tuning the wavelength of OPA and measuring the corresponding intensity of two-photon-excited fluorescence. The wavelength tuning of OPA and data collection were computer-controlled with a LabView routine. At each wavelength, the fluorescence intensity was normalized to the square of the excitation photon flux, measured in the reference channel. To exclude possible artifacts, for example, those caused by absorption at wavelengths close to the linear absorption, we checked that at each wavelength the fluorescence signal increased as a square of the excitation intensity.

Absolute 2PA cross sections were measured using the relative fluorescence technique at 650 nm excitation.[54] We used a bis-diphenylamino stilbene solution in DCM, for which $\sigma_2 = 250$ GM at 650 nm, as a standard.[55] To obtain absolute 2PA spectra in GM units, all relative 2PA spectra were calibrated to the known (at 650 nm) absolute cross-section value.

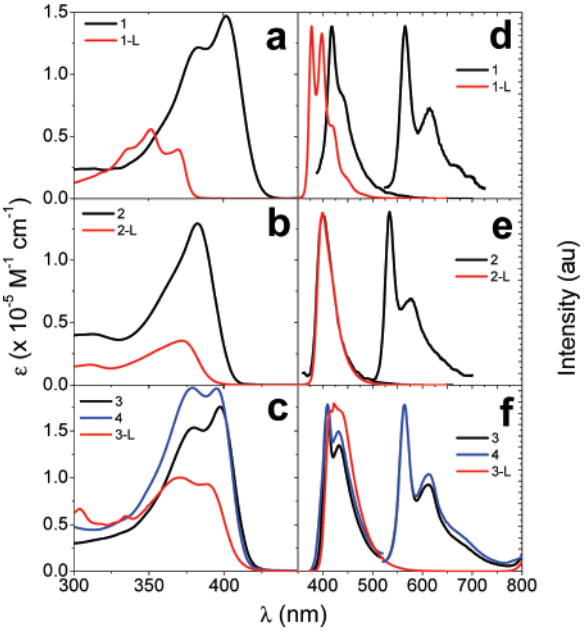

Figure 2. Quantified ground state absorption spectra of chromophores are shown in the left panels (a, b, and c). Data were obtained at room temperature (25 °C) in air-saturated benzene. The right panels (d, e, and f) are emission spectra obtained upon 330 and 370 nm excitation in benzene at room temperature for the ligands and Pt chromophores, respectively. Samples were either air-saturated (fluorescence) or deoxygenated (phosphorescence) via three freeze−pump−thaw cycles. No room-temperature phosphorescence was observed for **1-L**, **2-L**, and **3-L**.

Results

X-ray crystallography was accomplished for **1** and **2**. Details of these findings are also given in the Supporting Information. A notable structure result for compound **2** is that the angle between the fluorenyl carbon−nitrogen−phenyl carbon atoms is ~120°, showing that the lone pair of electrons on the nitrogen has sp^2 hybridization, resulting in conjugation with the fluorenyl group and the attached phenyls. The bond length of the acetylene bonded to the platinum atom is 1.208 ± 0.004 Å in compound **1**, but it is 1.144 ± 0.012 Å in compound **2**. This structural difference suggests that there is competition between backbonding from the platinum to the ligand and electron donation from the ligand to the platinum in the amino-substituted complex.

Ground-State Absorption. Quantitative ground-state absorption spectra for chromophores **1**, **2**, **3**, and **4**, along with ligands **1-L**, **2-L**, and **3-L** are shown in panels a, b, and c of Figure 2. Wavelength maxima and molar absorption coefficients are listed in Table 1. Each of the ligands exhibits a strongly allowed transition ($\epsilon > 4 \times 10^4$ M^{-1} cm^{-1}) in the near UV-region. Upon attachment of the ligands to the platinum centers in complexes **1**, **3**, and **4**, similar, but more intense, absorption bands appear that are red shifted with $\lambda_{max} \approx 395-400$ nm. The extinction coefficients follow the

(52) Turro, N. J. *Modern Molecular Photochemistry*; Benjamin/Cummings: Menlo Park, NJ, 1978.
(53) Murov, S. L.; Carmichael, I.; Hug, G. L. *Handbook of Photochemistry*, 2nd ed.; Marcel Dekker, Inc.: New York, 1993.
(54) Drobizhev, M.; Stepanenko, Y.; Dzenis, Y.; Karotki, A.; Rebane, A.; Taylor, P. N.; Anderson, H. L. *J. Phys. Chem. B* **2005**, *109*, 7223.
(55) Drobizhev, M.; Karotki, A.; Dzenis, Y.; Rebane, A.; Suo, Z.; Spangler, C. W. *J. Phys. Chem. B* **2003**, *107*, 7540.

Table 1. Summary of UV−vis Absorbance and Emission Data in Benzene

	Abs_{max}[a] (nm)	ϵ (M^{-1} cm^{-1})[b]	Fl_{max}[c] (nm)	E_S (eV)[d]	Φ_{fl}[e]	Ph_{max}[f] (nm)	Φ_{ph}[g]
1	402	147 000	418	3.03	0.017 ± 0.003	565	0.018 ± 0.002
2	383	129 000	399	3.18	0.010 ± 0.002	534	0.041 ± 0.003
3	397	176 000	409	3.08	0.038 ± 0.004	563	0.071 ± 0.005
4	397	192 000	409	3.08	0.037 ± 0.004	563	0.084 ± 0.007
1-L	351	55 800	377	3.30	0.692 ± 0.004		
2-L	372	35 400	399	3.22	0.741 ± 0.004		
3-L	371	100 000	422	3.14	0.710 ± 0.004		

[a] Absorption maximum. [b] Extinction coefficient. [c] Fluorescence maximum. [d] S_1 state energy. [e] Fluorescence quantum yield. [f] Phosphorescence maximum. [g] Phosphorescence quantum yield.

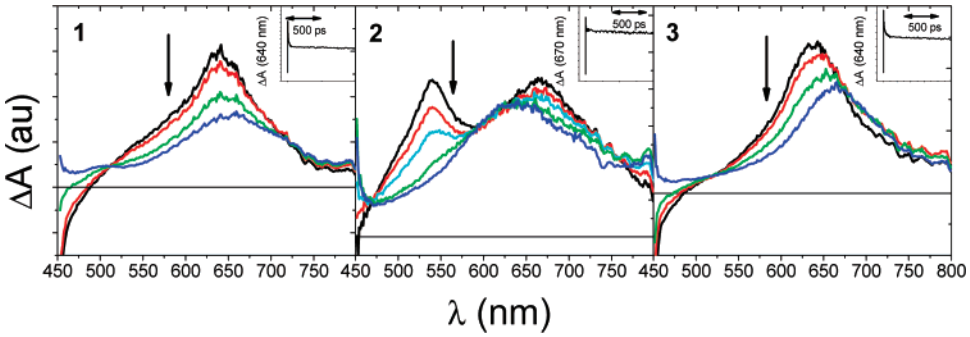

Figure 3. Femtosecond transient absorption spectra of **1** (32 μM), **2** (123 μM), and **3** (26 μM) in air-saturated benzene upon 400 nm excitation. Times shown are 0 (black), 1.5 (red), 3.4 (cyan, **2** only), 9.0 (green), and 48 ps (blue) after the 100 fs laser pulse. Similar spectral properties to **3** were observed for **4**. The chirp effect on the spectra were within experimental error, so no chirp corrections were made.

trends ϵ(**2**) < ϵ(**1**) < ϵ(**3**) < ϵ(**4**) and ϵ(**2-L**) < ϵ(**1-L**) < ϵ(**3-L**). The parallel trend between the complexes and ligands gives evidence for the $\pi\pi^*$ character in the optical transition. The ratio ϵ(complex)/(2ϵ(ligand)) measures the conjugation through the central platinum atom. When the ratio is larger than 1, there is significant conjugation through the platinum. When the ratio approaches 1, the optical transition has increased ligand-centered $\pi\pi^*$ character. The ratio follows the trend ϵ(**2**)/2ϵ(**2-L**) > ϵ(**1**)/2ϵ(**1-L**) >1 ≈ ϵ(**4**)/ϵ(**3-L**) ≈ ϵ(**3**)/2ϵ(**3-L**). Chromophores **1** and **2** show significant conjugation through the central platinum atom. The addition of the central diplatinum unit in chromophores **3** and **4** cause the optical transitions to be more ligand centered. The singlet-state energy of the ligands follows the trend E_S(**3-L**) < E_S(**2-L**) < E_S(**1-L**), while that of the platinum complexes follows the trend E_S(**1**) < E_S(**3**) ≈ E_S(**4**) < E_S(**2**). The magnitude of the red shift upon conversion of ligand to platinum complex follows the trend $|\Delta E_S(\mathbf{1})| > |\Delta E_S(\mathbf{2},\mathbf{3},\mathbf{4})|$. In each case, the red shift in the metal complexes signals that there is conjugation through the Pt−acetylide units. The red shift in chromophore **1** compared to that in ligand **1-L** is the largest of the series. This indicates that there is a greater extent of conjugation in the A−π−A complex **1** than in the D−π−D complexes **2** and **3**. The absorption spectra of **3** and **4** are very similar, with the only notable difference being that the absorption of the platinum dimer **4** is enhanced in the UV band at 380 nm. This enhancement is attributed to the Pt−C≡C−phenyl−C≡C−Pt unit which is known to absorb in this region.[56]

Emission. Panels d, e, and f in Figure 2 are the emission spectra of all the chromophores in benzene. For the Pt complexes both the normalized fluorescence (350−550 nm range) and room-temperature phosphorescence (550−750 nm range) under deoxygenated conditions are observed. Room-temperature phosphorescence was not observed from the ligands, as would be expected. Fluorescence and phosphorescence quantum yields are given in Table 1. The ligands all have high fluorescence quantum yields which decrease by a factor of approximately 30 upon formation of the platinum complex. When the fluorescence of the ligands is compared to that of the Pt complexes, it is interesting to note that the spectra of **2** and **2-L** are identical and that the spectra of **3**, **4**, and **3-L** are also similar. This is not the case for **1** and **1-L**. The spectra are quite different in shape, and the fluorescence from complex **1** is red shifted compared to that of ligand **1-L**. The phosphorescence of **2** is blue shifted compared to that of **1**, **3**, and **4**. Interestingly, the phosphorescence of the latter three overlap almost exactly, indicating that the triplet energies in these three complexes are nearly the same. Time-correlated single-photon counting (TCSPC) was used to measure the singlet-state lifetimes. For all of the platinum complexes, the emission decays well within the instrument response function of less than 50 ps, not providing useful information. The short lifetime of the fluorescence in the Pt complexes is consistent with intersystem crossing being very rapid ($k_{isc} \approx 10^{10}-10^{11}$ s^{-1}).

Transient Absorption. The femtosecond pump−probe technique was used to measure the S_1-S_n transient absorption spectrum of each compound and also to study the fast dynamics of relaxation. These data are shown in Figure 3 for **1**, **2**, and **3**. We also obtained time-resolved spectra for **4** but have not included them because they are nearly identical to those of **3**. Shown are transient spectra, obtained at various time delays ranging from immediately following

(56) Glusac, K.; Kose, M. E.; Jiang, H.; Schanze, K. S. *J. Phys. Chem. B* **2007**, *111*, 929−940.

Table 2. Summary of Transient Absorbance Data in Benzene

	1	2	3	4
S_1-S_{nmax}[a]	640 nm	540 nm	640 nm	640 nm
ϵ (M^{-1} cm^{-1})[b]	136 600	40 600	107 000	97 000
τ_S (air)[c]	23 ± 10 ps	42 ± 4 ps	48 ± 6 ps	12 ± 1 ps
T_1-T_{nmax}[d]	670 nm	610 nm	670 nm	670 nm
ϵ (M^{-1} cm^{-1})[e]	64 300	30 300	81 000	83 000
Φ_{ISC}[f]	0.95 ± 0.02	0.94 ± 0.03	0.92 ± 0.05	0.94 ± 0.01
τ_T (air)[g]	318 ns	44 ns	94 ns	99 ns
τ_T (deoxy)[h]	126 μs	117 μs	213 μs	238 μs

[a] Absorption maximum for the $S_1 \rightarrow S_n$ transition. [b] Extinction coefficient for the $S_1 \rightarrow S_n$ transition. [c] S_1 state lifetime. [d] Absorption maximum for the $T_1 \rightarrow T_n$ transition. [e] Extinction coefficient for the $T_1 \rightarrow T_n$ transition. [f] Intersystem crossing quantum yield. [g] T_1 state lifetime in the presence of air. [h] T_1 state lifetime in deoxygenated sample.

the laser pulse up to 48 ps after the pulse. For each chromophore, we observe biexponential decay kinetics. The lifetimes of the faster decay are 6.7 ± 0.5 (**1**), 4.8 ± 0.2 (**2**), 2.5 ± 0.3 (**3**), and 4.2 ± 0.2 ps (**4**) with the average fast decay time being 4.6 ps. We attribute the faster decay to internal conversion from higher singlet states, vibrational relaxation, and solvent reorganization about the molecule. The slower decay, having an average decay time of 31 ps, is assigned to intersystem crossing of the relaxed singlet state to the triplet state. The intersystem crossing lifetimes for this process are given in Table 2. A large shift in the transient spectrum associated with intersystem crossing is shown in Figure 3 for all materials. Compounds **1**, **3**, and **4** show a 25 nm red shift upon conversion to the triplet state. Compound **2** has anomalous behavior, with the initial excited-state absorption spectrum showing a 25 nm blue shift upon conversion and also an additional peak at 525 nm that disappears with time. In all cases, there is an isosbestic point, indicating the intersystem crossing involves interconversion between two species. The transient absorption spectrum appearing 48 ps after the 100 fs excitation is identical with that obtained in nanosecond laser flash photolysis experiments (described below), which confirms its assignment to triplet−triplet absorption. Further evidence that intersystem crossing takes place on a timescale of <50 ps can be found in TCSPC data. The singlet lifetimes obtained with this method were less than 50 ps (i.e., within instrument response) for all materials in air-saturated benzene, which is consistent with the ultrafast transient absorption data.

In the nanosecond transient absorption experiment, the triplet state is rapidly formed, then decays only slightly within the time scale limit of the ultrafast transient absorption (1.6 ns). The triplet lifetimes obtained with nanosecond laser flash photolysis under both air-saturated and deoxygenated conditions are presented in Table 2. Nanosecond transient absorption spectra are shown in Figure 4. Chromophores **1**, **3**, and **4** have maximum peaks at 670 nm, while **2** is blue shifted with a peak at 610 nm. The maximum molar absorption coefficient of **2** is less than one-half of that of the other chromophores. These values are given in Table 2. The triplet nature of the excited state was confirmed via oxygen quenching. Intersystem crossing quantum yields are listed in Table 2. All compounds undergo intersystem crossing with quantum efficiency near unity, consistent with the short singlet lifetimes.

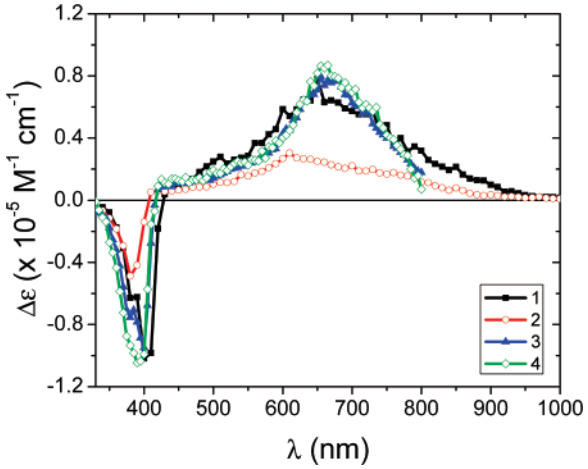

Figure 4. T_1-T_n absorption spectra observed after nanosecond-pulsed 355 nm excitation of **1** (5.9 μM), **2** (2.5 μM), **3** (3.0 μM), and **4** (1.7 μM) in deoxygenated benzene. Samples were deoxygenated by the freeze−pump−thaw method. Molar extinction coefficients were obtained by using the method of relative actinometry.

Two-Photon Absorption. Two-photon absorption spectra are presented in Figure 5. In general, all four compounds show a similar behavior. One may distinguish three distinct spectral regions: long, middle, and short wavelengths. In the long-wavelength region, $\lambda_{ex} > 850$ nm, 2PA gradually decreases toward long wavelengths. The middle region, around the one-photon absorption peak, has a moderately strong 2PA transition. The 2PA maximum almost coincides with the corresponding 1PA peak at $\lambda_{ex} \approx 2\lambda_{1PA}$. In the short wavelength region, $\lambda_{ex} = 600-700$ nm, a strong isolated 2PA peak shows up in all cases.

For quantitative comparison of the 2PA strength of our functionalized molecules with **PE2** and other analogs, we calculated an integrated 2PA strength of the short wavelength peak, which can be defined as $F = \int \sigma_2 \, d(2\nu)$, where ν is the laser frequency in cm^{-1}. These values, along with maximum 2PA cross-sections and spectral widths of the 2PA transitions, Γ_f, are collected in Table 3. We note here, that according to definition, the 2PA cross-section obtained with the relative fluorescence technique σ_2' is twice that obtained with nonlinear transmission methods such as *z*-scan:[3,24] $\sigma_2' = 2\sigma_2$. Therefore, for the sake of comparison, Tables 3 and 4 present all the data in terms of σ_2. As one can see, both the maximum value and the integrated strength of 2PA transition is greater for all compounds **1**−**4** compared to that of **PE2**.

Table 4 presents nonlinear absorption parameters relevant for higher-order multiphoton processes at a few selected wavelengths. The first two columns compare the effective 2PA cross-sections at 595 and at 720 nm measured in this work for **1**−**4** and those obtained in the literature for **PE2**. As one can see, all the compounds studied here greatly outperform **PE2** at 720 nm and show σ_2 of the same order or larger than **PE2** at 595 nm (see more details in Discussion). The next three columns of the table include the maximum triplet−triplet transient absorption cross-section (recalculated from data in Table 2), the width of the triplet−triplet absorption spectrum (Figure 4), and the triplet lifetime (Table 2). As one can see from Table 4, molecules **1**−**4**

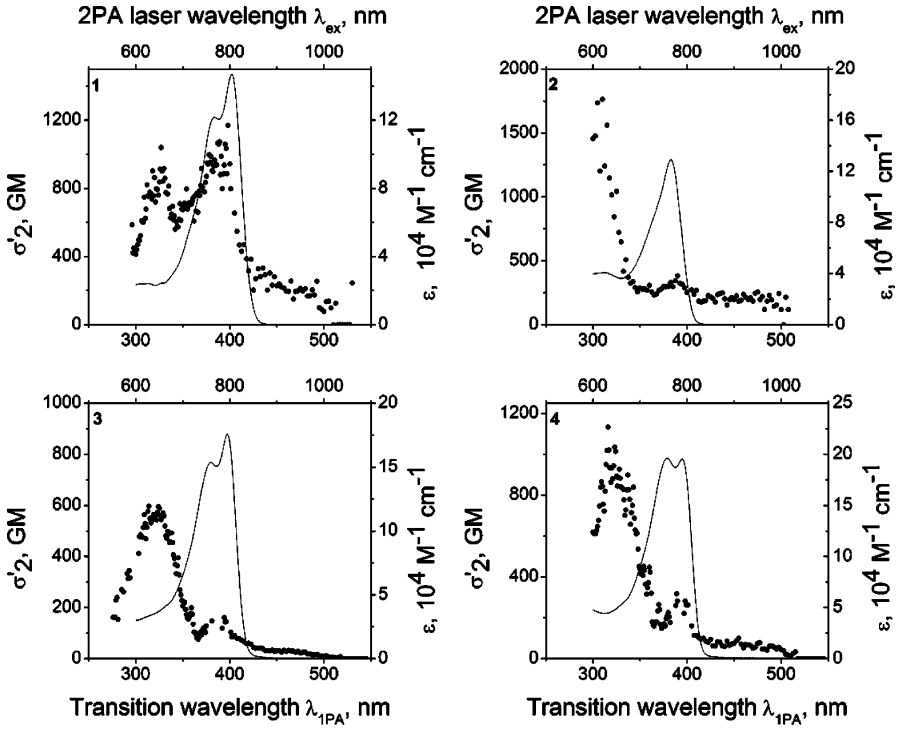

Figure 5. Two-photon absorption spectra of compounds **1**−**4** dissolved in benzene at ambient conditions. As described in the Experimental Section, the samples were excited with 100 fs pulses with $\lambda_{ex} = 550-1100$ nm. The absolute two-photon absorption cross-sections were measured using the sample fluorescence relative to a bis-diphenylaminostilbene solution in methylene chloride. This method gives the cross-section value σ'_2, which, according to definition, is twice that obtained with nonlinear absorption techniques ($\sigma'_2 = 2\sigma_2$).[3,24] One-photon absorption spectra (solid lines) are also shown for comparison. The bottom *x*-axis presents transition wavelength (which is equal to 1PA wavelength), and the top *x*-axis presents the laser wavelength used for 2PA excitation.

Table 3. Summary of 2PA Properties

molecule	$\sigma_{2,max}$[a]	$\lambda_{2PA,max}$[b]	Γ_f[c]	$\int\sigma_2\, d(2\nu)$[d]
1	415	649	4910	1.8×0^6
2	780	612	3570	2.5×10^6
PE1[e]	18.1	443	800[6]	1.5×10^4
3	290	634	4980	1.3×10^6
4	480	644	4540	2.0×10^6
PE1-amino[e]	90.2	495	800[f]	7.22×10^4
PE2[g]	235	595	~4000[g]	0.94×10^6
PE2[e]	37.6	457	800[6]	3.01×10^4

[a] Maximum 2PA cross-section (GM). [b] Wavelength of maximum 2PA cross-section (nm). [c] fwhm (cm^{-1}). [d] Integrated 2PA intensity (GM cm^{-1}). [e] Quantum-chemical calculation from Norman.[58] **PE1** is bis(phenylethynyl)bis(tributylphosphine)platinum(II). [f] fwhm, assumed value.[58] [g] From McKay.[42]

Table 4. Nonlinear Absorption Properties Relevant for Higher-Order Multiphoton Absorption Processes

	σ_2[a] (595 nm)	σ_2 (720 nm)	σ_1^{T-T} (λ_{max})[b]	$\Delta\lambda$[c]	τ_T[d]
PE2	235[e] (27 ps, *z*-scan)	7[f] (180 fs, *z*-scan)	2.2×10^{-16} (600)[g]	200[g]	42[g]
1	210 (100 fs, fluo)	370 (100 fs, fluo)	2.4×10^{-16} (670)	220	126
2	720 (100 fs, fluo)	140 (100 fs, fluo)	1.2×10^{-16} (610)	250	117
3	155 (100 fs, fluo)	60 (100 fs, fluo)	3.1×10^{-16} (670)	170	213
4	300 (100 fs, fluo)	160 (100 fs, fluo)	3.2×10^{-16} (670)	160	238

[a] 2PA cross-section (GM) at designated wavelength. [b] Triplet-state absorption cross-section (cm^2) at maximum absorption wavelength (nm). [c] fwhm of triplet-state absorption spectrum (nm). [d] Triplet-state lifetime of deoxygenated solution (μs). [e] Published data.[28] [f] Published data.[43] [g] Published data.[29]

possess a favorable set of parameters compared to **PE2**. A slightly lower σ_1^{T-T} value for **2**, compared to that of **PE2**, is greatly offset by a much larger σ_2 value, in addition to a wider T−T absorption.

Two-Photon Pumped Transient Absorption. To confirm the ability of **1**−**4** to populate the triplet excited-state via 2PA, a modified laser flash photolysis experiment was used. The data obtained are shown in Figure 6. The spectra for **1**, **3**, and **4** are identical to the spectra shown in Figure 4. The data obtained for **2** is very noisy, consistent with a triplet extinction coefficient less than half of that of the other compounds and a small two-photon cross-section at 803 nm resulting from the blue-shifted two-photon absorption maximum for this material. These results prove that, regardless of excitation mode (1PA or 2PA), ultimately, formation of the triplet excited-state is realized. Lifetimes obtained under these conditions are significantly shorter than those collected under one-photon excitation conditions seen in Table 2, as shown with compound **3** (3.5 vs 213 μs) and compound **4** (2.7 vs 238 μs). The one-photon excitation conditions involve dilute solutions(10^{-6} M), while the two-photon excitation conditions involve more concentrated solutions (0.02 M). We believe the decrease in lifetimes to be the result of a self-quenching mechanism, where an excimer forms between the excited chromophore and a ground-state chromophore. Self-quenching may contribute to the noisy data in compound **2**. This behavior has been observed in a similar Pt complex at higher concentrations than used in 2PA experiment.[57]

(57) (a) Connick, W. B.; Geiger, D.; Eisenberg, R. *Inorg. Chem.* **1999**, *38*, 3264. (b) Slagle, J. E.; Cooper, T. M.; Krein, D. M.; Rogers, J. E.; McLean, D. G.; Urbas, A. M. *Chem. Phys. Lett.* Submitted for publication.

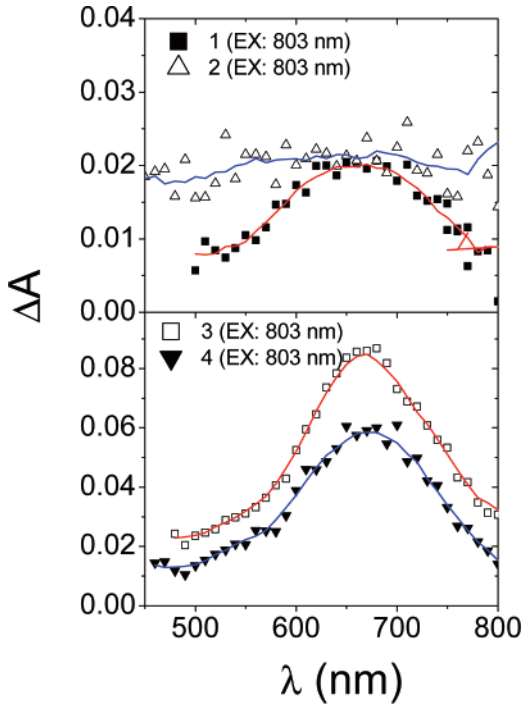

Figure 6. Examples of T_1-T_n absorption spectra produced by 5 ns, 803 nm pulsed excitation. All samples were prepared at 0.02 M in deoxygenated benzene. Deoxygenation was done with three freeze−pump−thaw cycles.

Discussion

Excited State Structure and One-Photon Photophysics. The ground-state absorption spectra of platinum acetylide complexes have been shown to be dominated by the allowed transition between the HOMO and LUMO levels. The transition is primarily $\pi\pi^*$ with metal-to-ligand charge transfer (MLCT) character.[58,59] The HOMO of platinum acetylides typically consists of a dπ orbital on the platinum center combined with π-symmetry orbitals on the ligands. The LUMO is centrosymmetric and is comprised exclusively of ligand-localized π^* orbitals, p orbitals on the Pt, and no contribution from dπ orbitals on the platinum atom. Given the highly delocalized nature of these orbitals, it is evident that the S_1 state is delocalized through the central platinum. As shown by the large increase in extinction coefficient when the free ligand is compared to the complex, the S_1 state in complexes **1** and **2** is strongly delocalized, while the smaller change in **3** and **4** suggest the S_1 state is more ligand centered.

A previous study of the homologous series of platinum acetylides **PE1**, **PE2**, **PE3**, and the analogous set of butadiynes and ligands gives a relation between end-to-end chromophore length and the singlet energy, E_S.[60] Using that relation and the end-to-end lengths of compounds **1**−**3**, we estimated their E_S values, and in all three cases, the relation overestimates the experimental E_S values by 0.1−0.2 eV. The largest difference (~0.2 eV) is in compound **1**. The difference between the previously studied chromophores and compounds **1**−**3** is the presence of the strongly conjugated units in the acetylide ligands. In particular, it is likely the high electron affinity of the benzothiazolyl group in compound **1** introduces intraligand charge-transfer character and delocalization of the S_1 state into the heteroaromatic ring system. The 4-(dialkylamino)phenylethynyl substituents on the fluorene ligand in **3** and **4** also provide increased π-conjugation in the S_1 state. The excited-state is comparatively more localized in **2**; although the amino substitutent is electron-donating and may introduce some charge-transfer character, the excitation is localized primarily on both the fluorene units and not the diphenyl amino groups, resulting in a relatively higher energy S_1 state in this complex.

In previous work, we demonstrated that the triplet exciton of platinum acetylides is localized on a single acetylide ligand.[56,59] In keeping with this concept, we believe that in the series of complexes **1**−**4** the triplet exciton is confined to a single ligand. In particular, the triplet energies (T_1) of the complexes, reflected by the phosphorescence emission band maxima, lie at ~2.20 eV in **1**, **3**, and **4** and at ~2.32 eV in **2**. As a point of reference, the triplet energy of 9,9-dihexylfluorene is 2.86 eV, and for an oligomer containing three 9,9-dihexylfluorene repeats, it is 2.25 eV.[61] This comparison indicates that the triplet exciton in all of the complexes is delocalized beyond the fluorene unit, likely extending into the ethynylene units, as well as into the additional aromatic ring systems in **1**, **3**, and **4**. Note that the phosphorescence spectra of **3** and **4** are superimposable, which underscores the fact that the triplet is localized in the more highly conjugated fluorenyl ligand system, rather than being localized in the [−Pt−C≡C−C_6H_4−C≡C−Pt−] region of the chromophore, which is known to have a triplet energy of 2.40 eV.[30] Interestingly, the triplet energy in **2** is higher than in the other complexes, and this is clearly caused by the reduced conjugation available in this complex's ligand system. Similar behavior is seen in the nanosecond transient absorption spectra, where compounds **1**, **3**, and **4** have the same maximum, while **2** has a blue shift, suggesting a smaller conjugation length in **2**. From the phosphorescence and intersystem-crossing to ground-state quantum yields for compounds **1**−**4**, the average radiative rate constant is $k_{ph} \approx 10^2\ s^{-1}$, while the average nonradiative intersystem crossing rate constant is $k_{isc}(T_1 \rightarrow S_0) \approx 10^4\ s^{-1}$. The nonradiative decay rate constant is similar to published results showing a relation between energy gap and decay rate.[62]

The femtosecond transient absorption spectra shown in Figure 3 provide a probe into the intersystem crossing process in the platinum acetylide chromophores. In all cases, initial excitation into the Franck−Condon S_1 excited state is followed by relaxation into the T_1 state within 48 ps after the 100 fs laser pulse. The short singlet-state lifetime in the Pt complexes is consistent with intersystem crossing being

(58) Norman, P.; Crostrand, P.; Ericsson, J. *Chem. Phys.* **2002**, *285*, 207.
(59) Cooper, T. M.; Krein, D. M.; Burke, A. R.; McLean, D. G.; Rogers, J. E.; Slagle, J. E. *J. Phys. Chem. A* **2006**, *110*, 13370.
(60) Rogers, J. E.; Hall, B. C.; Hufnagle, D. C.; Slagle, J. E.; Ault, A. P.; McLean, D. G.; Fleitz, P. A.; Cooper, T. M. *J. Chem. Phys.* **2005**, *122*, 214708.
(61) Wasserberg, S. P.; Dudek, S. P.; Meskers, S. C. J.; Janssen, R. A. J. *Chem. Phys. Lett.* **2005**, *411*, 273.
(62) Wilson, J. S.; Chawdrury, N.; Al-Mandhary, M. R. A.; Younis, M.; Khan, M.; Raithby, P. R. K., A.; Friend, R. H. *J. Am. Chem. Soc.* **2001**, *123*, 9412.

very rapid. This finding is in accord with the strong spin−orbit coupling induced by the heavy-metal Pt atom. As described in recent reviews of femtosecond absorption spectroscopy of transition metal complexes,[63,64] the processes occurring upon excitation include wave packet migration, intersystem crossing, and vibrational and solvent relaxation. In transition metal complexes, intersystem crossing can be very rapid because of the strong spin−orbit coupling induced by mixing of the ligand (π and π^*) and metal (dπ) orbitals. For example, the triplet state of excited $[Ru(bpy)_3]^{2+}$ appears within 100 fs,[65] while McCusker[64] describes solvent and vibrational relaxation occurring on a picosecond time scale. In the ultrafast transient absorption spectra of platinum acetylides **1**−**4**, spectroscopic changes are observed that are associated with initial excitation, vibrational cooling, solvent relaxation, and conversion to the relaxed T_1 state. From the measured singlet state lifetimes and intersystem crossing quantum yields, the intersystem crossing rates are in the range $k_{isc}(S_1 \rightarrow T_1) \approx 10^{10}-10^{11}$ s^{-1}, showing moderately efficient mixing of the S_1 and T_1 states. This behavior contrasts with that of the d^6 metal complex systems (e.g., $Ru(bpy)_3^{2+}$), where the singlet−triplet mixing is considerably stronger, and it is not possible to observe a distinct spectroscopic signature of a singlet state prior to intersystem crossing ($k_{isc} > 10^{12}$ s^{-1}). Finally, from the intersystem crossing and fluorescence quantum yields, we deduce that the rates of fluorescence decay and internal conversion are comparable ($k_{fl} \approx k_{ic} \approx 10^9$ s^{-1}).

An interesting point is that the ultrafast transient absorption spectra and dynamics observed for compound **2** are different than those of compounds **1**, **3**, and **4**. In particular, the transient spectrum immediately after excitation features bands at 525 and 675 nm. On a time scale of approximately 10 ps, the 525 nm peak decays, and the band in the red part of the spectrum blue shifts to 640 nm, with conversion complete within 30 ps. A possible explanation for this behavior can be found in a recent study of the ultrafast transient absorption dynamics of a triphenylamine chromophore.[66] In this paper, the authors report femtosecond transient absorption spectra of tris-4,4′,4″-(4-nitrophenylethynyl)triphenylamine, which initially features bands at 500 and 650 nm, followed by spectral evolution and dynamics which are quite similar to those observed for **2**. The authors conclude that the spectra arise because of relaxation of a Frank−Condon state that is completely delocalized through the C_3-symmetry triphenylamine chromophore, which undergoes rapid relaxation into a charge transfer state that is localized on a single C_1-symmetry conjugated unit. In complex **2**, a diphenylamino chromophore is attached to the fluorenyl group; thus, the ligand can be viewed as a fluorenyl-substituted triphenylamine chromophore. It is possible that in the Franck−Condon state of this complex the excitation is delocalized on the pseudo-C_3 symmetry triarylamine chromophore, and the relaxation that takes place on the picosecond time scale involves localization of the excitation into the fluorenylacetylide chromophore, followed by intersystem crossing to produce the triplet state. Evidence for the contribution of the triarylamine portion of the ligand to the Franck−Condon state can be found from the X-ray diffraction results for **2**, where the carbon−nitrogen−phenyl bond angle being 120° results in conjugation between the phenyl groups and the rest of the chromophore.

Two-Photon Absorption and Photophysics. The 2PA properties of some linear platinum acetylides were previously studied theoretically by Norman et al.[58] According to calculations, both centrosymmetric and noncentrosymmetric structures have a broad set of 2PA-allowed transitions in the visible part of the spectrum. One particularly strong transition occurring at an energy higher than the lowest 1PA transition dominates. Our data qualitatively reproduces this theoretical picture, especially if we consider that 2PA transition frequencies obtained from calculations are often higher than observed in the experiment.[58] A significant fact is that the very strong 2PA peak experimentally observed in the region $\lambda_{ex} = 600-700$ nm (see Figure 5) is universal for all four of the complexes, and it is not reproduced in the one-photon absorption (there are no isolated peaks at 300−350 nm in 1PA). This 2PA peak can be tentatively assigned to a one-photon-forbidden, but two-photon-allowed, gerade−gerade transition to the S_m state (Scheme 1). This, in turn, implies that the absorbing species possesses inversion symmetry and the Pt atom is involved in the conjugated system. The average S_m state energy is 3.91 eV. Is the S_m state different from the S_n state observed by femtosecond pump−probe spectroscopy? The average energy difference $E(S_m) - E(S_1) = 0.82$ eV, while the average energy difference $E(S_n) - E(S_1) = 2.02$ eV. This difference shows the S_m state is distinct from the S_n state.

All compounds also show a much weaker, but distinct, 2PA peak at $\lambda_{ex} = 750-800$ nm, which is nearly co-incident with the 1PA maximum. There are two possible explanations to this apparent violation of the alternative selection rule. First, both bands may be observed because of a different coupling of the electronic transition to non-totally symmetric vibrations in 1PA and 2PA. The second possibility is that in solution there are at least two different conformers, at least one of them being centrosymmetric, while the others are not. The first possibility (vibronic coupling) seems less probable because the observed 2PA band is moderately strong: $\sigma_2' \approx 150-300$ GM (1 GM = 10^{-50} cm^4 s) in **2** and **3** and even stronger (∼900 GM) in **1**. This should imply a non-realistically large change of permanent dipole moment (5−10 D) because of nonsymmetrical vibration. Also, such a violation of selection rules has not been observed in other one-dimensional centrosymmetric oligo-phenylene-vinylene family of molecules.[24] In noncentrosymmetric conformers, the large change of permanent dipole moment can be imagined if, because of breaking of symmetry, a Franck−Condon excitation is localized on one ligand. Therefore, we tentatively assign the 2PA peak near 750−800 nm to the presence of noncentrosymmetric conformers.

(63) Vleck, A., Jr. *Coord. Chem. Rev.* **2000**, *200*−*202*, 933.
(64) McCusker, J. K. *Acc. Chem. Res.* **2003**, *36*, 876.
(65) Cannizzo, A.; van Mourik, F.; Gawelda, S.; Zgrablic, G.; Bressler, C.; Chergui, M. *Angew. Chem., Int. Ed.* **2006**, *45*, 3174.
(66) Ramakrishna, G.; Bhaskar, A.; Goodson, T. *J. Phys. Chem. B* **2006**, *110*, 20872.

It is interesting to note that 1PA spectra of centrosymmetric and noncentrosymmetric conformers were predicted to have coinciding transition frequencies and almost the same oscillator strengths (cf. compounds **mIIb** and **mIIc** in Table 3 of Norman).[58] If our assumption about different conformers is correct, then 2PA spectroscopy can be uniquely suited for distinguishing between these species. On the other hand, the simultaneous presence of different types of conformers in the solution suggests that the 2PA strengths which are reported herein and are measured by the fluorescence technique, reflect perhaps not the true value but rather an effective weighted average of different conformer cross-sections.

For simplicity, suppose that there are two types of conformers: centrosymmetric (conformer 1) and noncentrosymmetric (conformer 2). One can show that the two have an identical fluorescence spectrum, both in shape and in quantum efficiency (which, according to our preliminary data seems to be the case for compounds studied here), then the measured effective 2PA cross-section at each particular wavelength λ_{ex} is

$$\sigma_2^{(\mathrm{eff})}(\lambda_{ex}) = n_1\sigma_2^{(1)}(\lambda_{ex}) + n_2\sigma_2^{(2)}(\lambda_{ex}) \qquad (3)$$

where indices 1 and 2 correspond to conformers **1** and **2** and n_i is equal to the mole fraction of the ith conformer, such that $n_1 + n_2 = 1$. Without independent knowledge of n_i values, we cannot estimate separately $\sigma_2^{(1)}$ and $\sigma_2^{(2)}$. On the other hand, if our assignment of the 2PA peaks is correct and because $n_i < 1$, each conformer will have an even larger maximum σ_2 value compared to that presented in Figure 5.

In the series of linear platinum acetylide multiphoton absorbers, **PE2** can be considered to be a convenient benchmark because it has been studied rather extensively.[28,42,43,58,67−73] Staromlynska and co-workers found the 2PA coefficient of **PE2** to be $\beta = 0.34$ cm/GW at 595 nm in 0.08 M solution.[28] By using the expression

$$\sigma_2 = \frac{\beta h\nu}{N_0 d} \qquad (4)$$

where N_0 is Avogadro's number and d is the concentration, this translates to 2PA cross-section equal to 235 GM. Since this value was obtained with the z-scan technique and 27 ps pulses, the authors do not exclude an excited-state absorption contribution, and thus $\sigma_2 = 235$ GM can be considered as an upper limit for the intrinsic 2PA cross-section. This assumption finds further confirmation in the recent data of Vestberg et al., who obtained $\sigma_2 = 7$ GM at 720 nm for **PE2** by using the z-scan technique and much shorter 180 fs pulses.[43] The 2PA cross-section value of **PE2** at 720 and 595 nm can also deviate because of its substantial dispersion, but according to McKay et al., the 2PA spectrum is very broad and almost flat in the region of 580−690 nm.[67] With all this information taken into account, a reasonable estimation of the intrinsic **PE2** 2PA cross-section would be several tens of GM near 595 nm.

Even though our data present only a lower limit and those of McKay et al. present an upper limit for σ_2, one can clearly see that all the molecules studied in the present work show substantially higher 2PA intensity (as presented in the last column of Table 3) than **PE2**. We do not present the data of Vestberg et al. in Table 3 because their σ_2 value does not correspond to 2PA maximum. Molecules **3** and **4** possess at least 1.4 and 2 times, respectively, stronger 2PA, first, because substitution of phenyls with fluorenyls increases conjugation. Also, they carry symmetrically attached electron-donating alkylamino groups, which were shown to drastically increase 2PA because of symmetrical charge transfer in the first excited state.[16] For platinum acetylide compounds, this effect was demonstrated theoretically,[58] where diamino substitution increased the 2PA strength of **PE1** by 5 times (cf. compounds **PE1-amino** and **PE1** in Table 3). It is also worth comparing **PE2** with **1** and **2**. While the number of ethynyl bonds decreases in **1** and **2**, the replacement of phenylethynyl group at each side of **PE2** with benzthiazolylfluorenes and diphenylaminofluorenes in **1** and **2**, which represent strong electron acceptors or donors, repectively, and also the replacement of phenyl linker with more highly conjugated fluorene linker results in at least 2 and 3 times enhancement of integrated 2PA in **1** and **2**, respectively.

Summary and Conclusions

The design of new two-photon absorbing chromophores coupled with Pt complexes to produce materials that exihibit large intrinsic 2PA cross-sections, coupled with efficient intersystem crossing to afford long-lifetime triplet states, has proven successful in this study. This investigation has focused on the synthesis and photophysical characterization of a series of platinum acetylide complexes that feature highly π-conjugated ligands substituted with π-donor or -acceptor moieties. The conjugated ligands impart the complexes with effective two-photon absorption properties, while the heavy-metal platinum centers give rise to efficient intersystem crossing to afford long-lived triplet states. Photophysical studies demonstrate that one-photon excitation of the chromophores produces an S_1 state that is delocalized across the two conjugated ligands, with weak (excitonic) coupling through the platinum centers. The S_1 state is observed by ultrafast transient absorption and by its characteristic fluorescence. Intersystem crossing occurs rapidly ($k_{isc} \approx 10^{11}$ s^{-1}) to produce the T_1 state, which is believed to be localized on a single conjugated fluorenyl ligand. The

(67) McKay, T. J.; Bolger, J. A.; Staromlynska, J.; Davy, J. R. *J. Chem. Phys.* **1998**, *108*, 5537.
(68) Staromlynska, J.; McKay, T. J.; Wilson, P. *J. Appl. Phys.* **2000**, *88*, 1726.
(69) McKay, T. J.; Staromlynska, J.; Davy, J. R.; Bolger, J. A. *J. Opt. Soc. Am. B* **2001**, *18*, 358.
(70) Cooper, T. M.; McLean, D. G.; Rogers, J. E. *Chem. Phys. Lett.* **2001**, *349*, 31.
(71) Cooper, T. M.; Blaudeau, J.-P.; Hall, B. C.; Rogers, J. E.; McLean, D. G.; Liu, Y.; Toscano, J. P. *Chem. Phys. Lett.* **2004**, *400*, 239.
(72) Silverman, E. E.; Cardolaccia, T.; Zhao, X.; Kim, K.-Y.; Haskins-Glusac, K.; Schanze, K. S. *Coord. Chem. Rev.* **2005**, *249*, 1491.
(73) Parola, S.; Ortenblad, M.; Chaput, F.; Desroshes, C.; Miele, P.; Baldeck, P. L.; Malmstrom, E.; Lindgren, M.; Eliasson, B.; Ericksson, A.; Lopes, C. *SPIE Proc.* **2005**, *5934*, 1.

triplet state is strongly absorbing ($\epsilon_{TT} > 5 \times 10^4\ M^{-1}\ cm^{-1}$), and it is very long-lived ($\tau > 100\ \mu s$).

Femtosecond pulses were used to characterize the 2PA properties of the complexes, and as expected, all of the chromophores are relatively efficient two-photon absorbers in the visible and near-infrared region of the spectrum (600−800 nm). The complexes exhibit maximum 2PA at a shorter wavelength than 2λ for the 1PA band, consistent with the dominant 2PA transition arising from a two-photon-allowed gerade−gerade transition. Nanosecond transient absorption experiments carried out on several of the complexes with excitation at 803 nm confirm that the long-lived triplet state can be produced efficiently via a sequence involving two-photon excitation to produce S_1, followed by intersystem crossing to afford T_1.

Acknowledgment. We are thankful for the support of this work by AFRL/ML Contracts F33615-99-C-5415 for D.G.M., F33615-03-D-5408 for D.M.K., and F33615-03-D-5421 for J.E.R. and J.E.S. We thank Evgeny Danilov and Prof. Michael Rodgers for use and help with the femtosecond transient absorption experiment at the Ohio Laboratory for Kinetic Spectrometry located at Bowling Green State University. We also thank Dr. Ramamurthi Kannan and Dr. Loon-Seng Tan at AFRL/MLBP for providing us with the ligands used for chromophores **1** and **2**. Rebane's group at Montana State University was supported by AFOSR Grants FA9550-05-1-0357 and FA9550-05-1-0236. K.S.S. and K.Y.K. acknowledge AFOSR for support by Grant FA-9550-06-1-1084.

Supporting Information Available: Complete synthesis procedures, analytical data, NMR data, and X-ray crystallographic files (CIF) of compounds **1** and **2**. This material is available free of charge via the Internet at http://pubs.acs.org.

IC700549N